

REPORT DOCUMENTATION PAGE			Form Approved OMB NO. 0704-0188		
<p>The public reporting burden for this collection of information is estimated to average 1 hour per response, including the time for reviewing instructions, searching existing data sources, gathering and maintaining the data needed, and completing and reviewing the collection of information. Send comments regarding this burden estimate or any other aspect of this collection of information, including suggestions for reducing this burden, to Washington Headquarters Services, Directorate for Information Operations and Reports, 1215 Jefferson Davis Highway, Suite 1204, Arlington VA, 22202-4302. Respondents should be aware that notwithstanding any other provision of law, no person shall be subject to any penalty for failing to comply with a collection of information if it does not display a currently valid OMB control number. PLEASE DO NOT RETURN YOUR FORM TO THE ABOVE ADDRESS.</p>					
1. REPORT DATE (DD-MM-YYYY) 30-03-2020		2. REPORT TYPE Final Report		3. DATES COVERED (From - To) 1-Aug-2017 - 31-Dec-2019	
4. TITLE AND SUBTITLE Final Report: Unsteady Freestream Velocity Oscillation System at Rotorcraft-Relevant Mach Amplitude			5a. CONTRACT NUMBER W911NF-17-1-0379		
			5b. GRANT NUMBER		
			5c. PROGRAM ELEMENT NUMBER 611102		
6. AUTHORS			5d. PROJECT NUMBER		
			5e. TASK NUMBER		
			5f. WORK UNIT NUMBER		
7. PERFORMING ORGANIZATION NAMES AND ADDRESSES Ohio State University 1960 Kenny Road Columbus, OH 43210 -1016			8. PERFORMING ORGANIZATION REPORT NUMBER		
9. SPONSORING/MONITORING AGENCY NAME(S) AND ADDRESS (ES) U.S. Army Research Office P.O. Box 12211 Research Triangle Park, NC 27709-2211			10. SPONSOR/MONITOR'S ACRONYM(S) ARO		
			11. SPONSOR/MONITOR'S REPORT NUMBER(S) 70030-EG-RIP.3		
12. DISTRIBUTION AVAILABILITY STATEMENT Approved for public release; distribution is unlimited.					
13. SUPPLEMENTARY NOTES The views, opinions and/or findings contained in this report are those of the author(s) and should not be construed as an official Department of the Army position, policy or decision, unless so designated by other documentation.					
14. ABSTRACT					
15. SUBJECT TERMS					
16. SECURITY CLASSIFICATION OF:		17. LIMITATION OF ABSTRACT		15. NUMBER OF PAGES	19a. NAME OF RESPONSIBLE PERSON
a. REPORT UU	b. ABSTRACT UU	c. THIS PAGE UU	UU		James Gregory
				19b. TELEPHONE NUMBER 614-292-5024	

RPPR Final Report

as of 08-Apr-2020

Agency Code:

Proposal Number: 70030EGRIP

Agreement Number: W911NF-17-1-0379

INVESTIGATOR(S):

Name: Jeffrey Bons
Email: bons.2@osu.edu
Phone Number: 6142478414
Principal: N

Name: James W. Gregory
Email: gregory.234@osu.edu
Phone Number: 6142925024
Principal: Y

Organization: **Ohio State University**

Address: 1960 Kenny Road, Columbus, OH 432101016

Country: USA

DUNS Number: 832127323

EIN: 316025986

Report Date: 31-Mar-2020

Date Received: 30-Mar-2020

Final Report for Period Beginning 01-Aug-2017 and Ending 31-Dec-2019

Title: Unsteady Freestream Velocity Oscillation System at Rotorcraft-Relevant Mach Amplitude

Begin Performance Period: 01-Aug-2017

End Performance Period: 31-Dec-2019

Report Term: 0-Other

Submitted By: James Gregory

Email: gregory.234@osu.edu

Phone: (614) 292-5024

Distribution Statement: 1-Approved for public release; distribution is unlimited.

STEM Degrees:

STEM Participants:

Major Goals: To upgrade of the Ohio State University 6" x 22" Unsteady Transonic Wind Tunnel to provide advanced capabilities to carry out fundamental research. This facility is a novel U.S. asset and the upgrade will ensure that testing in this facility generates data of high quality for DoD research interests.

The P.I., Professor James Gregory, of the Ohio State University will use the equipment to augment and enhance research capabilities in the area of fluid dynamics, specifically the dynamics of unsteady and separated flows

Accomplishments: Several major upgrades to the existing equipment were acquired with the awarded funds, including structural modification of the wind tunnel and modernization of the wind tunnel operating platform, manufacturing elliptical choke vanes for Mach oscillation experiments, purchase of a miniature pressure scanner with improved pressure range, load pins that directly measure airfoil loads, upgrade of the data acquisition system, upgrade of the existing PIV system, and a high speed scientific camera with quadruple spatial resolution. These major purchases and upgrades together improve the capability and accuracy to capture transient air loads and flow phenomena, as well as enhanced the spatial and temporal resolution of the acquired data. Table 1 of Appendix A provides an itemization of equipment and services acquired with the grant funds.

Training Opportunities: The procured equipment has seen strong use by students in our group and can also benefit other projects not tested in this wind tunnel. The students have benefited from hands-on experience with these advanced optical measurement systems as they investigate a variety of unsteady fluid dynamic problems now possible with increased spatial and temporal resolution.

Results Dissemination: Nothing to Report

Honors and Awards: Nothing to Report

Protocol Activity Status:

**Unsteady Freestream Velocity Oscillation System at
Rotorcraft-Relevant Mach Amplitude**

Final Progress Report

ARO Grant W911NF-17-1-0379

Covering the Period

August 1, 2017 – December 31, 2019

Prepared for

U.S. Army Research Office

Attn: Dr. Matthew Munson

P.O. Box 12211

Research Triangle Park, North Carolina 27709

March 28, 2020

Prepared by

James W. Gregory

Jeffrey P. Bons

The Ohio State University

Aeronautical and Astronautical Research Laboratories

Aerospace Research Center

2300 W. Case Road, Columbus, Ohio 43235

With support from graduate students:

Wenbo Zhu and David Pitts

1. Introduction

Upgrade of the wind tunnel facility including structural modification, data acquisition system, and optical measurement technology has been made using the awarded funds to improve research capability of unsteady compressible fluid dynamics, including dynamic stall and unsteady airfoil loading in response to surging flow. This report contains an itemization of the acquired equipment and services as well as a summary of latest research projects benefitting from this upgrade. High-speed images of background-oriented schlieren (BOS) method involving an airfoil under surging flow are presented to demonstrate the improved capabilities of the facility. This case study demonstrates the successful upgrade of the wind tunnel structure to allow high quality optical measurement and improved data acquisition capability.

With the delivery of the new equipment, work is underway to investigate the effects of time-varying free-stream velocity on unsteady blade loads in the Ohio State University Unsteady Transonic Wind Tunnel. The key impact of this DURIP-funded instrumentation upgrade is improving the unsteady flow conditions in the wind tunnel operation, the accuracy and consistency of time-resolved flow visualization utilizing techniques such as particle image velocimetry (PIV) and BOS, and the unsteady calculation of airfoil loads. The procured instrumentation and system upgrade to the wind tunnel has demonstrated benefits to current and future DoD-funded research investigations into unsteady compressible fluid dynamics, as well as dynamic stall.

2. Procured Equipment

Several major upgrades to the existing equipment were acquired with the awarded funds, including structural modification of the wind tunnel and modernization of the wind tunnel operating platform, manufacturing elliptical choke vanes for Mach oscillation experiments, purchase of a miniature pressure scanner with improved pressure range, load pins that directly measure airfoil loads, upgrade of the data acquisition system, upgrade of the existing PIV system, and a high speed scientific camera with quadruple spatial resolution. These major purchases and upgrades together improve the capability and accuracy to capture transient air loads and flow phenomena, as well as enhanced the spatial and temporal resolution of the acquired data. Table 1 of Appendix A provides an itemization of equipment and services acquired with the grant funds.

Wind tunnel structural modification

Current military aircraft cruise at 130 KIAS (Mach 0.2) while the Sikorsky X2 demonstrated a cruise capability of over 200 KIAS (Mach 0.3) and the proposed requirements document for the Army's Future Vertical Lift (FVL) program suggest a desired cruise speed greater than 230 KIAS (Mach 0.35). In order to capture the flow physics present on the flight vehicles being developed for the FVL vision, wind tunnel testing of high freestream Mach number and oscillating Mach amplitudes are needed.

The OSU Unsteady Transonic Wind Tunnel is a unique facility that has the potential to achieve these flow conditions. However, when the tunnel was operated at these high Mach amplitudes, significant longitudinal oscillations of the entire wind tunnel facility were experienced. This is the most fundamental limitation of the wind tunnel due to the unsteady momentum exiting the tunnel. These longitudinal oscillations, which are found to exacerbated at higher Mach number, higher Mach oscillation amplitudes, and higher Mach oscillation frequencies, can cause structural fatigue

on critical components such as the high-pressure supply line. Clearly, this becomes a safety issue that limits the operational envelope of the tunnel. In addition, the movement of the entire wind tunnel facility creates challenges for optical alignment of sensitive instrumentation such as PIV lasers that cannot sustain such oscillations. As a result, the accuracy of time-resolved optical measurements is limited.

In order to improve the safety and operational envelope of the wind tunnel, as well as to improve the flow diagnostics capability, structural modification of the wind tunnel has been made. The local engineering firm Barber & Hoffman, Inc. surveyed our facility and came up with solutions based on our requirements. The modification of the wind tunnel structure includes additional welding and bolting on the settling chamber existing members, transferring vibrational loads to the ground of the building with additional slab, beam, and channel braces (see Figure 1a and b), and adding angle kicker braces to help stabilize the high-pressure supply line and transfer lateral load into the roof structure (see Figure 1c).



Figure 1: Structural stabilization to the wind tunnel to mitigate longitudinal vibration: a) before stabilization, b) stabilization of the settling chamber, c) stabilization of the pressurized air supply line.

In addition, because the wind tunnel test section is made of aluminum, test section wall flexing occurs during wind tunnel operation. Prior to this project, wall flexure had been temporarily mitigated with additional steel clamps holding the side walls, see Figure 2a. This is improved in

this structural modification by replacing metal clamps with horizontal steel angles along each side of the assembly and welded to the steel beam flanges. Steel shims with elastomeric pads are placed between the steel and aluminum to adequately brace the wall and provide separation of dissimilar materials, see Figure 2b.

After this structural modification, the wind tunnel was tested several times for various steady and unsteady flow conditions. Both pressure and optical measurements have shown a significant improvement as wind tunnel vibration is mitigated. Investigation shows that the structural resonance frequency of the wind tunnel is shifted from around 10 Hz before this modification to about 20 Hz after the modification. The maximum recorded longitudinal translation of the facility had been approximately 1 inch, and is now also significantly reduced. Thus, this upgrade greatly benefits sensitive time-resolved flow visualizations such as PIV and BOS experiments.

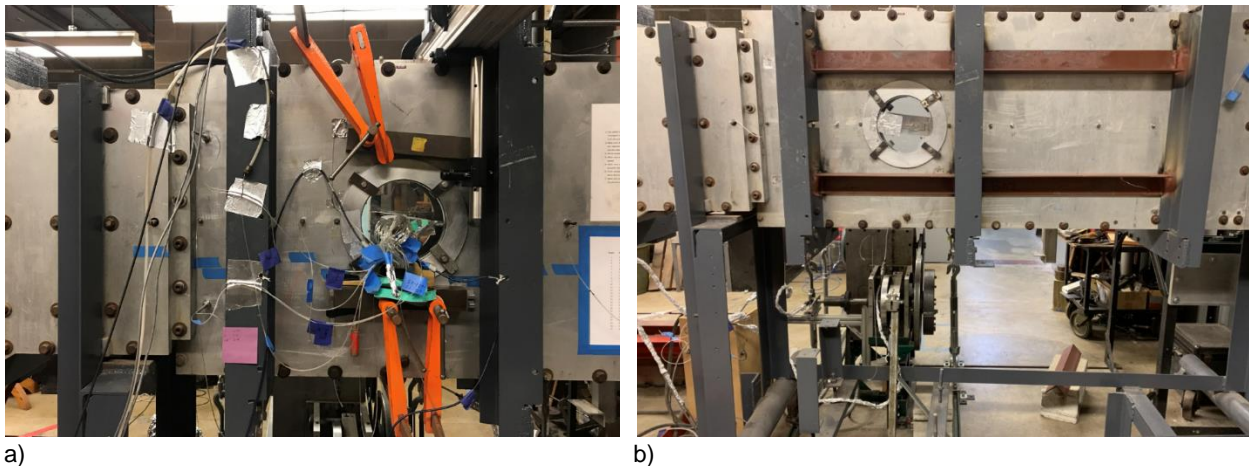


Figure 2: Structural reinforcement on the wind tunnel test section: a) test section before the modification, b) test section after the modification.

Another upgrade of the wind tunnel is a modernization of the facility operating platform. It is intended to create a safe, efficient, and effective work environment for tunnel operators. The comparison of this upgrade is shown in Figure 3. The major changes include reorganizing equipment and wires relating to operating the wind tunnel, allowing remote access to wind tunnel data acquisition (analog data and optical measurements) and real-time wind tunnel feeds (with three webcams of 1040p and 30 Hz around the facility), and providing emergency power and stop to the tunnel operation for the safety of the personnel and facility. These changes allow for all personnel to remain in the control room (a much safer position), rather than being positioned alongside the wind tunnel for data acquisition.



a)



b)

Figure 3: Upgrade of the wind tunnel operation control platform, a) before the upgrade, b) after the upgrade.

Mach oscillation choke vanes

Time-varying free-stream Mach number is achieved by rotating elliptical choke vanes downstream of the test-section. The test-section Mach number can be predicted reasonably well by the isentropic area-Mach relationship (*i.e.*, A/A^*). The choke area is established with a set of four elliptical vanes with a geometry described by $(x/a)^m + (y/b)^n = 1$, where x and y are super-ellipse coordinates in the Cartesian coordinate system, a is the semi-major axis, b is the semi-minor axis, m and n are parameters controlling the elliptical profile to match a sinusoidal Mach number. Components of one choke vane assembly are shown in Figure 4.

Two sets of elliptical choke vanes for a mean Mach number of 0.2 and amplitude of 0.05 and 0.1 were 3D printed. The 3D printing sample has proven to be much more economic in both cost and manufacturing time compared to the CNC mill. In addition, due to the greater blockage area corresponding to the lower test-section Mach number, the choke vane volume is about four times of the previous mean $M = 0.4$ choke vanes. This leads to a significant increase in the inertia of

the vanes and the power required of the motor driving them if aluminum choke vanes are used. As a result, 3D printing choke vanes are desired for the Mach number in the current experiments. Two additional choke vanes are manufactured as backup parts. So far, these parts have shown consistency for over a hundred of operations.



Figure 4: 3D printed elliptical choke vane for Mach oscillation.

Pressure scanner

Airfoil surface pressure measurement is the primary method used in our tunnel for airfoil unsteady load measurements. Our prior installation involved surface pressure taps that were connected to two ESP 32HD pressure scanners (Figure 5) via flexible tubing of 1.5 mm in diameter and approximately 20 cm long. A hardware-triggered DTC Initium interface reads in the multiplexed analog output of the scanners at 1 kHz and streams the data to a dedicated hard disk. The scanner system is thermally compensated to minimize zero and span shifts. The pressure scanners are triggered by a TTL pulse train to ensure a harmonized sample interval and accurate temporal correlation with other instrumentation. The dynamic response of this measurement technique is suitable for these unsteady measurements since the tubing length is short and dynamic compensation is applied to the signals.

The current installation has three pressure scanners with a range of 30 psia. This pressure range was selected in order to optimize data accuracy at lower Mach numbers. However, as the Mach amplitude is increased there are elevated dynamic pressures that exceed the measurement range of these transducers. In addition, these two pressure scanners also measure additional pressure information along the tunnel, such as settling chamber pressure, test-section freestream static and stagnation pressures, airfoil downstream stagnation pressures, etc. Thus, the number of pressure taps on the airfoil is also limited by the available ports on the scanner.

Under this grant, we added one additional pressure scanner in order to shorten the length of the pressure tubing, and to increase the total number of pressure taps possible on the airfoil. A 50 psia range was selected for additional 32-channel module. The existing DTC Initium interface can handle the additional module in parallel with the existing modules, bringing the total channel count up to 96 simultaneous samples at 1 kHz.

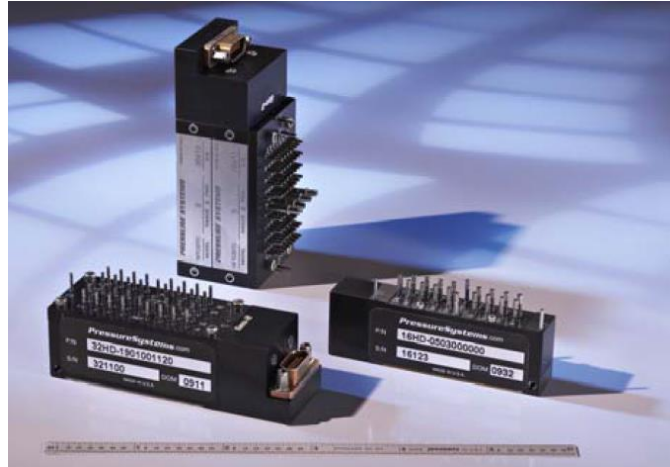
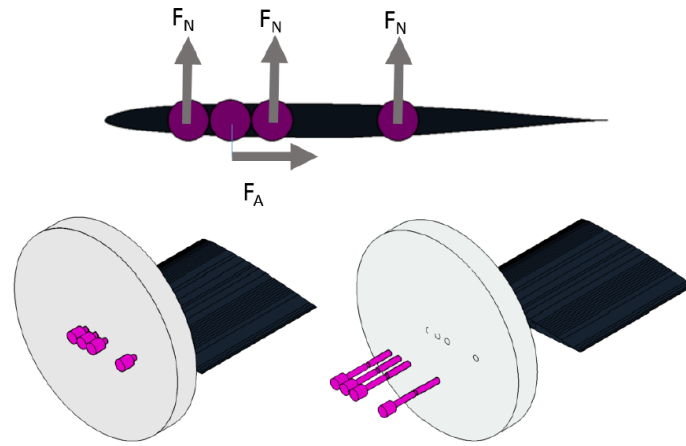


Figure 5: Miniature electronic pressure scanner.

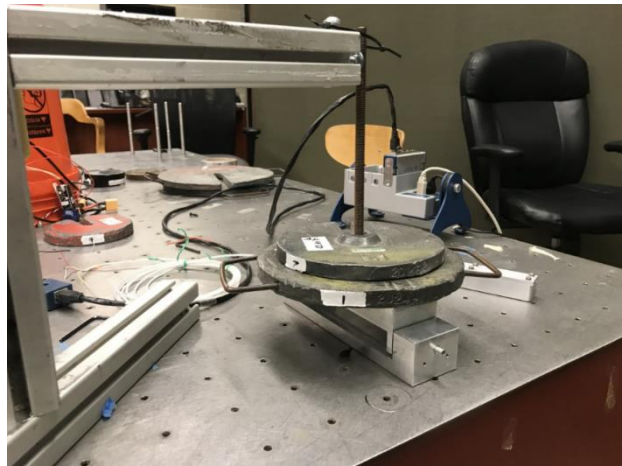
Load pins

As stated above, airfoil load measurements are achieved through surface pressure taps located on both suction and pressure surfaces. However, due to the test section size, test articles are limited in size relative to other wind tunnels which leads to reduced pressure tap resolution near the leading edge and trailing edge of the airfoil. Experimentally, this results in limited fidelity of pressure data surrounding the airfoil leading and trailing edge which translates to loading coefficients that deviate from experimental results collected at similar conditions in other tunnels. In addition, the sole reliance on pressure data produces unrealistic drag calculations due to the absence of sensors to capture viscous drag.

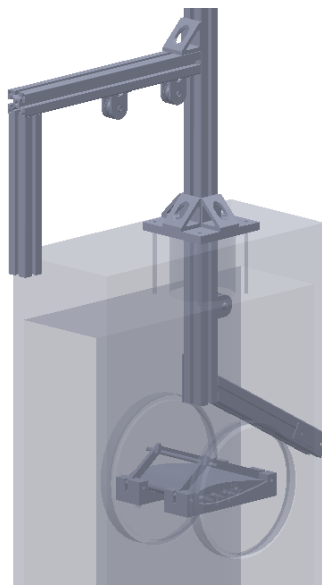
As a result, a load cell is required to directly measure lift, drag, and moment. Multiple single-axis 0.23" diameter Strainsert™ shear load pins suspending the airfoil from the tunnel and oriented in the normal or axial direction of the chord are selected. With precisely known locations the normal and axial forces can be used to compute actual lift, drag, and moment acting upon the airfoil. The Strainsert load pin signal bandwidth can produce data at rates up to 100 kHz. Each load pin has a load capacity of 50 lb. and 1% full scale measurement accuracy. The configuration of load-pin airfoil assembly is shown in Figure 6a, where three load pins are used to measure the normal force and one load pin is used to measure the axial force. However, the orientation of load pin direction can be rearranged conveniently to compensate for different test conditions. The benchtop calibration of a single load-pin is shown in Figure 6b, data has demonstrated good repeatability and match with factory measurements. However, the airfoil (and load-pins) installed in the wind tunnel test section experience different configurations than the benchtop calibration. As a result, an in-situ calibration is needed for the application of load-pin in wind tunnel experiments. This is an ongoing progress which graduate students are working on. The current design of the load-pin in-situ calibration is shown in Figure 6c.



a)



b)



c)

Figure 6: Airfoil load measurements with load pin: a) configuration of shear load pins with the airfoil, b) benchtop calibration, c) design of wind tunnel in-situ calibration

DAQ system upgrade

The original data acquisition (DAQ) system involves two National Instruments (NI) devices, BNC-2120 and 2121, to collect analog inputs and synchronization of signals of the wind tunnel experiments. Because of the limited channels and signal types available, additional electronic components are added, leading to a cluttered and inefficient overall data acquisition system, shown in Figure 7a. In addition, with the newly procured equipment, such as load-pins, the existing data acquisition system is not sufficient to capture all types of data without significant modifications.

To solve this dilemma, a latest NI compactRIO (cRIO) system with NI-DAQmx is selected to replace the old data acquisition system. The cRIO-9047 has a 1.6 GHz quad core processor, 4GB RAM and 4GB storage, and 8 slots for NI C-series modules that adapt to changing measurement and control requirements. To satisfy the needs of measurement and control in our wind tunnel facility, various NI modules are selected. A NI 9212 with isothermal terminal block is used to measure up to 8 thermocouple signals at 24-bit and up to 95 samples per second per channel. This is used to measure the stagnation temperature in the settling chamber and any additional temperature information in future experiments. A NI 9215 with BNC connectors and a NI 9215 with screw terminals are used to measure voltage signals from different sensors, such as from an Omega pressure transducer. It is capable of 100 kilo-samples per second per channel at 16-bit for 8 channels. This is a significant improvement of the number of voltage signals and sampling rate from the original system. Another module is the NI 9237 with Dsub connector. This module provides strain or load measurements with zero inter-channel phase delay. It includes all the signal conditioning required to power and measure up to four bridge-based sensors simultaneously, such as four load-pins procured in this grant. The maximum sample rate is 50 kilo-samples per second per channel. Since our wind tunnel is used for unsteady compressible flow research, three quadrature encoders are used to measure oscillatory behaviors experienced in the experiments. The encoder signals can be sampled by two NI 9361 counter input modules. Each module can support two quadrature incremental encoders at 32-bit. These two counter input modules are used to replace the whole BNC-2121 and lab-made circuit board, greatly simplify the DAQ setup. The last module is NI 9263 with voltage output to trigger other devices such as optical measuring devices (camera, laser, etc.). Together, the new data acquisition system (cRIO and C-series modules) can sample all existing data with improved capabilities and allow for growing data acquisition needs in the future.

The new DAQ system is mounted on a server rack cabinet, along with power supplies and emergency power backup battery is shown in Figure 7b. This more compact and powerful DAQ system helps improve the data acquisition robustness and accuracy. Additional testing to support other newly procured equipment is under way.



a)



b)

Figure 7: Data acquisition of the wind tunnel experiment: a) before the modification, b) after the modification.

PIV system upgrade

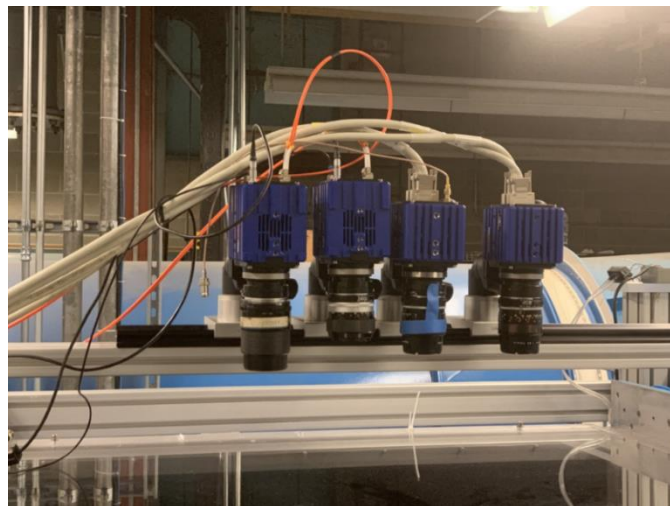
A PIV system from LaVision, Inc. was purchased about a decade ago. The CCD cameras from this purchase lack sufficient pixel resolution to clearly resolve details of flow features in our recent wind tunnel experiments or other recent lab projects. In addition, the post-processing capability of PIV or other optical measurements is limited by the software package and computing power of this old system. A typical recent wind tunnel optical measurement (e.g. PIV) of one test case with 15,000 images of 1280 x 800 pixels led to 24 hours of post-processing, significantly suppressing the working efficiency of this type of measurement. Thus, upgrade of the existing PIV system is necessary to improve work efficiency and to take advantage of modern updates of relevant technologies.

The upgraded PIV system was purchased from a single vendor (LaVision, Inc.) after a thorough price comparison among all vendors (Dantec Dynamics Inc. and TSI Inc.) and

consideration of compatibility with existing PIV system components (also from LaVision, Inc.). In addition, educational discounts that met or exceeded those offered to the U.S. government were granted in the final purchase.

The final PIV upgrade includes the following items. Two 5.5 mega-pixel scientific CMOS (sCMOS) cameras with camera link HS frame grabber and fiber optic link cable are procured to replace the old CCD cameras, see Figure 8a. They have a maximum spatial resolution of 2560 x 2160 pixel at 50 Hz. They can be used for low-speed stereoscopic PIV in lab projects. Two new dual-plane dual-sided (DPDS) calibration targets are also acquired. The smaller one (204 x 204 mm) can fit into the Ohio State University Unsteady Transonic Wind Tunnel for PIV calibration, whereas the larger one (309 x 309 mm) can be used for other fluid dynamics projects. In order to improve the post-processing power of optical measurements, the existing DaVis software licenses are upgraded to DaVis 10. Furthermore, GPU processing for DaVis software package is added to accelerate the image processing. The latest tests have shown a significant improvement in post-processing, reducing aforementioned 24-hour window down to 5 hours with the PIV upgrade. The last upgrade is on the programmable timing unit (PTU). The new PTU-9 allows variable trigger delay for phase-resolved measurements. These upgraded items (except the sCMOS cameras) are assembled into a mobile image processing workstation (Figure 8b), allowing for convenient setup between different experiments in the lab.

Final delivery of PIV system components was taken on late November 2019 and additional support materials were delivered in December 2019. In the ensuing months, the system was assembled and verified in increasing levels of complexity. Full-scale time-resolved PIV and stereo-PIV measurements will be taken in the wind tunnel in the near future.



a)



b)

Figure 8: PIV system upgrade components: a) upgraded duo sCMOS cameras, two on the left. b) upgraded optical data processing workstation, include upgraded DaVis software, GPU processing capability, upgraded PTU, etc.

High-speed camera

With the increased capability of optical measurements in our wind tunnel (due to mitigated tunnel vibration and upgraded image processing power) and the recent application of the BOS method in studying the surging flow phenomenon, it naturally becomes demanding to improve the capability of the high-speed camera for the last piece of the optical measuring system. The high-speed camera owned in the lab is the Phantom v1210, which has a maximum spatial resolution of 1280 x 800 pixels and 12,000 fps at this full resolution. It was a relatively powerful camera when it was purchased years ago. However, for the size of the optical access and the size of the test article in our wind tunnel, a measurement of the full flow field around the airfoil during dynamic stall or surging flow will lead to significant decrease in spatial resolution. As a result, only a small window of flow field can be sampled for meaningful data analysis.

Due to this limitation, a new high-speed CMOS camera is procured to supplement the requirement of improved spatial resolution in optical measurements. The Phantom VEO 440 (Figure 9) is chosen which has a maximum spatial resolution of 2560 x 1600 pixels, quadruple the resolution of the Phantom v1210. The maximum sample rate is 1100 fps at full resolution, satisfying current experimental requirements. In addition, the 10Gb Ethernet data transfer capability is added to significantly reduce the time of data transfer. Tests have shown that

transferring a 72 GB of image data, typical for one dataset from the tunnel experiment, has reduced from 30 mins using the previous system to about only 2 mins.



Figure 9: 4-megapixel high-speed scientific camera VEO-440 (Vision Research Inc.).

3. Support of Proposed Research

Part of the acquired equipment has already been implemented to support the ongoing surging flow study in our laboratory. Students supported by this specific project while gaining experience with the advanced instrumentation include two graduate students, one of whom is studying for Ph.D.

The OSU Unsteady Transonic Wind Tunnel has served as the primary test facility for ARO-related projects. This unique facility is capable of several dynamic modes, *i.e.* unsteady freestream (surging flow), dynamic stall with pitching motion, and coupled surging-pitching motion. Because flow is choked at downstream of the test section, Reynold number and Mach number can be varied independently within the operating limit. For the current project, elliptical choke vanes are used to generate time-varying freestream velocity while the airfoil is held at a constant angle of attack. Unsteady airfoil loads measured from surface pressure taps give unsteady lift coefficient and is compared with the classic unsteady airfoil theory.

Due to the mitigated tunnel vibration and upgrades of optical measuring devices, the BOS method is utilized at the moment to study time-resolved flow structures and to explain corresponding lift response. To demonstrate improved data acquisition capabilities, a time-resolved BOS of a NACA 0018 airfoil with free-stream Mach oscillations is presented. For the test case discussed below, the airfoil was set to a 4° angle of attack and the freestream Mach oscillation frequency was 3.5 Hz. The mean Mach number was 0.2, with a peak of 0.25 and minimum near 0.15. Chord Reynolds number was 1.5 million.

The BOS method is an optical density visualization technique that measures the deflection of light rays caused by changes in the local index of refraction. The index of refraction is related to the density that exists in a fluid, such as air, based on the Gladstone-Dale relation. The BOS method utilizes this principle by observing a randomly generated speckle pattern in the background of the medium. The experimental setup consists of an imaging system, a background speckle pattern, an external light source, and a volume of fluids with density gradients. Unlike the regular schlieren method, the imaging system (camera) is focused on the dotted background pattern in the BOS method. When a density gradient is present in the medium, light is refracted

and the speckle pattern in the image will be displaced compared to that without density gradients. This displacement of the background pattern when light rays are refracted is analogous to moving particles in PIV. As a result, the displacement of the speckle pattern is an indicator of the density gradient.

In this experiment, the high-speed Phantom CMOS camera VEO-440 with a 200 mm, $f/4$ Nikon lens is placed on one side of the optical window, shown in Figure 10. The camera is placed 0.47 m away from the center of the wind tunnel test-section and the lens is set as $f/32$ for the optimal depth of field. Images are taken at 500 fps, with a spatial resolution of 2560 x 1600. the high-speed camera is triggered the same way as the pressure signals. On the other side of the test section lies the speckle pattern and a 14,000 lumen LED array. The background speckle pattern is attached to a clear acrylic plate and is illuminated by the LED array from the back. A reference image without any flow in the tunnel is first taken for every test and is compared to the images taken when the compressed air is supplied to the wind tunnel. By cross correlating the wind-off and the wind-on images, a local displacement of speckle pattern in pixels can be quantified at each frame, with the pixel displacement being proportional to the density gradient integrated along the line of path. The processing of the BOS images is done with the commercial software DaVis 10 utilizing the same cross-correlation technique used in PIV. In this work, the camera field of view is zoomed in on the trailing edge region of the airfoil. An image showing the field of view is displayed in Figure 11.



Figure 10: Experimental setup of the BOS technique for Mach oscillation measurements.

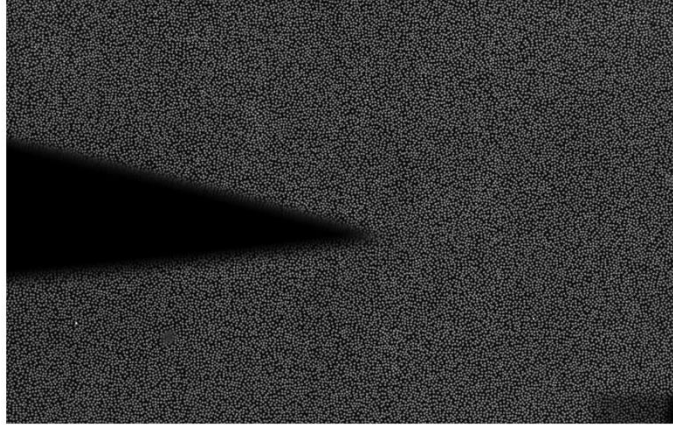


Figure 11: Field of view of the background speckle pattern.

The BOS method is intended to visualize the effects of viscous phenomena near the airfoil trailing edge and study the Kutta condition under unsteady free stream. The viscous boundary layers and wake shear layer are expected to produce density gradients due to shear layer vorticity, viscous dissipation, and heat transfer. It is expected that the boundary layers on the upper and lower surfaces should each produce a density gradient of opposite sign, and these viscous layers should merge at the trailing edge. A line of zero density gradient, denoted as the wake centerline, should form downstream of the trailing edge. Thus, minimum density gradient is expected at the centerline of the wake, which is indeed observed in the pixel displacement field in Figure 12.

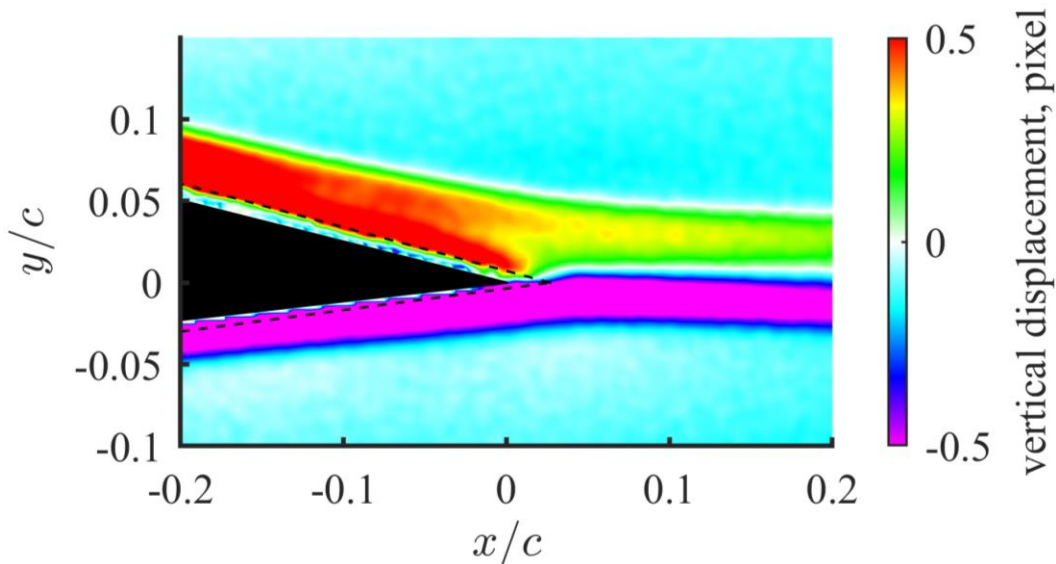


Figure 12: Displacement (density gradient) field of BOS experiments processed with DaVis software.

In Figure 12, the airfoil trailing edge is masked in black. A dashed line adjacent to the airfoil indicates the extent of image blur around the airfoil surface. In this work, only the vertical displacement field are shown. The key feature extracted from the BOS data is the location of the wake centerline as a function of downstream distance, referenced to the trailing edge. A more detailed study of the unsteady wake behavior can be done by considering only the wake centerline data. For the current dataset, more than 90 oscillation cycles are phase averaged with a 15 Hz low-pass filter. For each phase position, the locus of points corresponding to minimum density

gradient is extracted from each BOS image and plotted in Figure 13, along with the corresponding steady stagnation streamlines. The movement of the trailing edge stagnation streamline under surging flow is clearly observed, with the stagnation streamline deflected upwards from 270° to 0° . At other phase positions, the stagnation streamline follows more closely to the path of the steady stagnation streamline. It is found that the phase positions where the stagnation streamline deflect upwards correspond to the phase angles where the lift coefficient is low relative to the quasi-steady value, whereas when the position of the wake centerline is similar to or below the steady case, the unsteady c_l is greater than steady c_l .

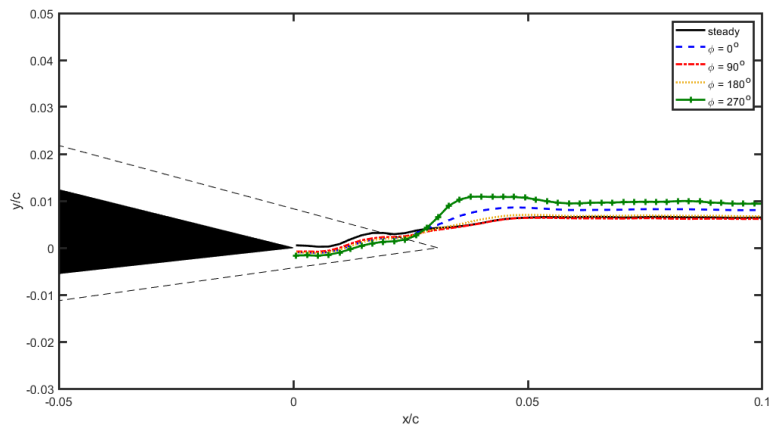


Figure 13: Oscillations of trailing edge stagnation streamline under surging flow.

The time-resolved BOS data analysis demonstrates unsteady Kutta condition for the NACA 0018 at high Re in a low frequency, incompressible, low angles of attack flow condition. This violation of steady Kutta condition used in classic unsteady airfoil theory helps enlighten the difference observed in our recent experimental measurements with the theory. With the upgrade procured in this award, further study can be achieved to explore this surging flow characteristics such as PIV measurements of the whole flow field and direct lift measurements using load-pins.

4. Conclusions and Future Work

The services and instrumentation procured under the awarded DURIP funds have added powerful spatial and temporal resolution to measurements of unsteady flow phenomena in a range of applications relevant to the DoD mission, with a major emphasis on compressible unsteady free stream for rotating blades. As the wind tunnel structure, analog data acquisition, and high-speed PIV/BOS system are optimized for routine use, the equipment setup will be used to explore a range of scientific problems of interest to the DoD. The first deployment of the BOS system has yielded results which qualitatively and quantitatively capture the unsteady trailing edge stagnation streamline oscillations associated with unsteady lift coefficient frequency response. The procured equipment has seen strong use by students in our group and can also benefit other projects not tested in this wind tunnel. The students have benefited from hands-on experience with these advanced optical measurement systems as they investigate a variety of unsteady fluid dynamic problems now possible with increased spatial and temporal resolution.

Appendix A: Inventory of Procured Equipment

Table 1: Itemization of procured equipment and service using award funds.

Item	Description	Model/Article No.	Manufacturer	Cost (USD)
Four (4) sets of 3D-printed Choke Vanes	A total of 16 3D-printed elliptical Choke Vanes forming 2 sets and 2 backups, used to generate 2 different Mach oscillation profiles in the Unsteady Transonic Wind Tunnel	-	OSU Department of Mechanical and Aerospace Engineering Machine Shop	\$4,954.32
Four (4) Load Pins	Clevis Pin, 50-lb Capacity, 0.7-mV/V (NOM), 350 ohms, Type W, plus retaining rings	Q25161	STRAINSERT Co.	\$8,117.89
One (1) Miniature High-Speed Pressure Scanner Brick	32 channels silicon piezoresistive sensors per brick with thermal compensation; max 1,200 samples/sec per scanner; -12 to 30 PSID, $\pm 0.03\%$ full-span accuracy, plus 5 ft cable	ESP-32HD	Measurement Specialties, Inc.	\$11,677.86
Data Acquisition/Control Modules for Wind Tunnel DAQ Upgrade	NI cRIO-9047, 1.6 GHz quad-core, 4 GB RAM, 4 GB Storage, Kintex-7 70T FPGA, 8-slot, with 8 modules for analog voltage, temperature, counter, etc. inputs and outputs	cRIO-9047	National Instruments	\$18,746.10
Servo Drive for Wind Tunnel DAQ Upgrade	Kollmorgen brushless servo position indexer, 24 A continuous output, 240 VAC 3 phase input, with EtherCAT connection	AKD-P02406-NBCC-0000	THAL-MOR ASSOCIATES, Inc.	
Servomotor for Wind Tunnel DAQ Upgrade	Kollmorgen brushless servomotor	AKM73P-KKCNC-00	THAL-MOR ASSOCIATES, Inc.	
Wind Tunnel Operation Control Console	59" dual sit/stand console	Impulse B3263	WINSTED Corporation	\$8,774.00
Wind Tunnel Structure Modification Engineering	Professional Services include field visits, structural review, and drawing to stabilize the wind tunnel structure, mitigate wind tunnel axial vibration during operation	-	BARBER & HOFFMAN CONSULTING ENGINEERS	\$21,841.00
Wind Tunnel Structure Modification Labor	Furnish labor and equipment to install reinforcing material on wind tunnel	-	Steel Erectors International, Inc.	
Two (2) PIV Imager sCMOS Cameras	5.5 Megapixel scientific CMOS camera with global shutter and double-frame mode for PIV, spatial resolution of 2560 x 2160 pixel at 50 Hz	1101407	LaVision, Inc.	\$88,619.00

PIV GPU Processing for DaVis	Combined with multicore high-end video card for accelerated processing, include software integration in DaVis and support for 2D and Stereo PIV image processing and Tomo PIV volume reconstruction	1105230	LaVision, Inc.	
PIV Software Upgrade to DaVis 10.X	Software upgrade for existing license 11878 for 2D PIV, 3D PIV, self-calibration, etc.	1105325	LaVision, Inc.	
PIV Hardware	Other hardware includes camera link HS frame grabber, fiber optic link cable, Scheimpflug camera lens adapter, flow seeder, calibration target, programmable timing unit for DaVis 10.X	1108926	LaVision, Inc.	
4 Mega Pixel High-Speed Camera	2560 x 1600 pixel at 1100 fps, 72GB RAM, 10Gb Ethernet data transfer, plus power supply and cable	VEO-440L	Vision Research	\$41,540.00
DAQ computer	Titan S422 Octane – Intel Xenon	S422	Titan Computers	\$6,926.64
Miscellaneous Supplies & Services	Supplies and services to support listed items	-	McMaster-Carr, APC by Schneider Electric, United Sensors Corporation, Omega Engineering, etc.	\$3,930.22
Equipment total				\$215,127.03
Proposal Budget Total				\$215,163.00